Influence of Oxidation on Fatigue Crack Growth, on the Modelling of Thermal Fatigue Cracking

F. REZAI-ARIA* and L. REMY

Centre des Matériaux de l'Ecole des Mines de Paris, URA CNRS DO250, BP. 87, 91003 Evry Cedex, France

**Now with Ecole Polytechnique Fédérale de Lausanne, CH 1015 Lausanne, Switzerland*

ABSTRACT

The thermal fatigue behaviour of Mar M509, a cast cobalt-based superalloy, was previously shown to involve mainly crack propagation which is strongly influenced by oxidation. Crack propagation was modelled using damage equations which were based on a local approach and which took into account load ratio effects. Local stresses ahead of the crack were estimated from Tracey's finite element analysis of plane strain small scale yielding which was adapted to cyclic loading using Rice's hypothesis. High temperature oxidation of precracked CT specimens gave rise to alloy embrittlement at medium temperatures ahead of the oxidized precrack. The critical stress to fracture was found to increase with increasing distance from the oxidized crack tip and to depend on oxygen concentration. Damage equations were then introduced for thermal fatigue crack growth. These equations were used to compute the crack growth law in wedge specimens submitted to thermal fatigue. Good agreement was observed between experiment and prediction.

INTRODUCTION

During operation, turbine blade and vane materials in aircraft engines are submitted to severe cyclic thermal stresses in a highly oxidizing environment. In a take off and landing cycle, the critical parts of a blade are subjected to maximum stress at medium temperatures, Fig.1, [Rezai-Aria, 1986]. At high temperatures, where oxidation plays a major role, stresses are mainly compressive. Thermal fatigue (T.F.) gives rise to the oxidation of the material ahead of the crack tip at high temperatures and loading at medium temperatures damages by fatigue the material which was altered by oxidation.

Many authors have tried to describe the interactions of low cycle fatigue at high temperature (HTLCF) and creep [Manson, 1973] or oxidation [Coffin 1973, Reuchet and Rémy 1983]. Recently, the validity of these two approaches in HTLCF and TF data was discussed for Mar M509, a cobalt based superalloy, considering physical damage mechanisms. The oxidation models were shown to give more reliable life predictions than the creep models [Rémy *et al.*, 1988]. TF damage in such superalloys results from a synergistic effect of fatigue and oxidation and this has to be accounted for by life prediction models.

It was previously shown that the primary interdendritic MC carbides (tantalum rich) were preferentially oxidized and were responsible for early crack initiation in HTLCF and in TF of Mar M509 [Rezai-Aria *et al.*, 1988 a]. TF of this superalloy, was previously shown to involve mainly crack propagation which was strongly influenced by oxidation [Rezai-Aria *et al.*, 1988 a].
The aim of this study was to model crack propagation in Mar M509 under TF loading. A fatigue crack growth equation was introduced in the absence of any environmental influence using compact tension (CT) specimens. The influence of high temperature oxidation on fatigue crack growth at medium temperatures was studied using precracked CT specimens which were oxidized at high temperature and then loaded at medium temperatures. Damage equations were derived to describe the synergistic effects of oxidation and fatigue under T.F. loading as well as under HTLCF loading [Rezai-Aria, 1986].

EXPERIMENTAL PROCEDURE

Material

Mar M509 is cast cobalt-based superalloy used for vanes in jet engines. The chemical composition of the master heat used in this study was the following in weight percentage : 0.59C - 11Ni - 23.2Cr - 6.95W - 3.3Ta-0.30Zr - 0.22Ti - 0.17Fe - 0.008B - 0.005P - 0.003S - bal.Co. All specimens were heat treated for 6h at 1230°C. Special castings were made in which two TF wedge specimens could be machined (the average grain size is 0.8mm).

Thermal fatigue specimens and test conditions

One wedge specimen 55mm in length and with 0.25mm wedge radius (type A) was used, Fig.1. The influence of specimen geometry on the TF behaviour has been discussed previously [Rezai-Aria *et al.*, 1988 a]. The TF tests were carried out on a rig of SNECMA. The specimens were uniformly heated along their thin edge by the flame of a burner using a mixture of air and propane gas for about 60s and then they were cooled by compressed air for 20s. Two thermal cycles were studied between 200 and 1100°C and between 200 and 950°C. The evolution of the major crack was monitored using test interruptions and surface inspections under optical microscopy. Every experiment was duplicated.

Fatigue crack growth tests on preoxidized specimens

As mentioned above, during a TF cycle, oxidation plays a major role at high temperature while the stress is negligible or compressive. Maximum tensile stresses occur at intermediate temperatures, Fig.2. An original procedure was used to simulate the material alteration by oxidation. CT specimens were first precracked to a/w = 0.4 at 600°C where there are no oxidation effects. These specimens were then oxidized in a furnace at 900°C for 300h. The interdendritic oxide depth (lox) previously measured [Reuchet and Rémy, 1983] for this condition was 32.5 μm.

These precracked and oxidized specimens were then cycled at the lower temperature under increasing loading steps. The tests were started using a small load range (ΔK about a few $MPa.m^{1/2}$). Each new loading step was started when crack growth slows down.

RESULTS AND DISCUSSION

Fatigue crack growth in preoxidized specimens

A typical experiment at 600°C (after 300h oxidation at 900°C) is shown in Fig.3, and compared with FCGR curve of the virgin material (i.e. without any previous oxidation at 900°C). FCGR was much higher than in the virgin material. Then a step increase in the load gives rise to a large growth rate which then slows down. This was repeated under successive step load increases and a saw - tooth FCGR curve was so produced with maximum rates up to 10 or 100μm/cycles until FCGR decreased down to the value observed in the virgin material. A material zone ahead of the previous crack tip was thus altered (embrittled) by oxidation (on almost 1 mm in the quoted experiment). Such experiments were carried out at 400, 500, 600 and 900°C.

We propose a model based on local stresses in a volume element at the crack tip (using a local approach to fracture) to explain this material behaviour.

Damage equation for fatigue in absence of oxidation

In a local approach a volume element ahead of the crack tip cracks when a local fracture criterion is reached [Mc Clintock, 1963]. Such types of models for fatigue crack growth were recently reviewed and discussed [Chalant and Rémy, 1983]. In stage III, where the high FCGR becomes strongly dependent of the load ratio $R(= K_{min}/K_{max})$, there is a superposition of fatigue damage and of static fracture modes such as cleavage or ductile fracture [Knott, 1973]. Fracture was assumed to obey a maximum principal stress criterion in this low ductility alloy as shown for cleavage in steels [Beremin, 1983]. Therefore an empirical mathematical expression was used to describe fatigue fracture of a microstructural element at high FCGR as follows :

$$1/N(\lambda) = (\Delta\sigma_{eq}/2So)^{M} / [(1 - R) \times (\sigma_c - \sigma_{yy})/So]^{\alpha} \qquad (1)$$

with $R = \langle 1 - (\Delta\sigma_{yy}/\sigma_{yy}) \rangle$

where $\langle u \rangle$ is zero if $u<0$ and u if $u > 0$, and where So, M, σ_c and $\alpha(=2.4)$ are constants for a given temperature. σ_{yy} is the maximum tensile value of the normal stress ahead of the crack tip at a distance λ.

Local stresses were derived from the finite element analysis of plane strain-small scale yielding by Tracey [1976] and averaged over a square microstructural element at the crack tip (λ = 100 μm i.e. the average secondary dendrite size) as detailed elsewhere [Chalant and Rémy, 1983, Rezai-Aria, 1986]. FCGR were measured on CT specimens for two load ratio R = 0.1 and R = 0.6 at 400, 500, 600 and 900°C. Fig.4 shows the influence of the R ratio on a plot $\Delta\sigma eq/2$ versus $N(\lambda)$ at 600°C. Fig.5 presents $\Delta\sigma eq/2$ as a function of $N(\lambda)/[(1 - R) \times (\sigma_c - \sigma_{yy})]^{\alpha}$ for the same data. Eq.1 was, by this way, fitted to FCGR at different temperatures. In this way this equation was able to describe FCGR including the R ratio effect using four parameters, So, M, σ_c, and $\alpha(=2.4)$ for a given temperature.

Damage equation for fatigue crack growth in preoxidized CT specimens

The critical stress to fracture, σ_c, could be deduced from Eq.1 for the preoxidized CT specimens. The various coefficients involved in this

equation were assumed to be the same for an oxidized material as well as for a virgin material. $N(\lambda)$, number of cycles to break a micro structural element at the crack tip, was deduced as $N(\lambda) = \lambda/(da/dN)$. Fig.6, shows the critical stress, σ_c , at 600°C as a function of the distance to the crack tip which has been normalized by the interdendritic oxide depth, lox. The critical stress, σ_c , increases very slowly over a distance about 20 times lox and then it increases more rapidly until it approaches the critical stress value of the virgin material when the crack leaves the zone embrittled by oxygen. This zone could be about 15 to 30 times larger than the oxide depth (lox $\cong$ 32.5 μm), i.e. about 0.5 to 1 mm. Quantitative measurements of oxygen concentration were made using the electron microprobe and have shown an exponential decrease of concentration with the distance (X) along interdendritic areas ahead of the oxidized precrack, Fig.7, [Rezai-Aria, 1986]. Such a relationship for a given oxidation treatment had been shown to be in agreement with Fisher's model for intergranular diffusion [Fischer, 1951].

The exponential variation of critical stress with the distance from the oxidized crack reflects its variation with oxygen concentration ahead of the crack tip. An empirical equation was used for the variation of σ_c with the distance :

$$\sigma_c = \sigma_{co} \, (1 - u + u \exp(m.X/l_{ox})) \qquad (2)$$

where m is a constant (equal to 0.1) and u and σ_{co} are two constants at a given temperature (with $|u| < 1$). This empirical equation means that the critical stress to fracture decreases when the oxygen concentration increases. This equation should apply provided that X is such that σ_c is smaller than the value for the virgin material σ_c^* . Eq.2 describes the variation of the critical stress to fracture with depth ahead of oxide using three parameters at a given temperature. FCGR in a preoxidized cracked specimen can be described using Eq.1 and Eq.2 together which involve a total of seven parameters at a given temperature. In this case fatigue fracture occurs after oxidation. However isothermal as well as thermal fatigue involve oxidation and fatigue at the same time. In the latter case Eq.1 and 2 can be used to model this complex interaction.

Oxidation fatigue damage equations for thermal fatigue crack growth

It is possible now to compute the FCGR under cyclic loading in an oxidizing environment with the knowledge of oxygen concentration as a function of time and distance ahead of the crack tip and of the local loading conditions of the volume element at the crack tip. Thermal fatigue wedge specimens are quite complex structures. Computation of the local loading conditions is more difficult than for LCF,but the stress computed for the uncracked structure could be used to account for short crack length in TF loading conditions. The application of these local fatigue fracture criteria under oxidation fatigue interaction will be tested using the stress computed for uncracked structures. TF wedge specimens were computed in a uniaxial approximation [Rezai-Aria *et al.*, 1988 b]. Therefore the damage equations were written for the uniaxial case but can be readily extended to multiaxial conditions (at least to proportional loading).

Under an oxidizing environment and cyclic loading an incremental damage, dD, will be introduced in a volume element ahead of the crack tip during one cycle. This increment of damage is given by Eq.1 which under uniaxial loading conditions reduces to :

$$dD = (\Delta\sigma/2So)^M / [(1 - R) \times (\sigma_c - \sigma) / So]^\alpha \qquad (3)$$

with $R = \langle 1 - (\Delta\sigma/\sigma) \rangle$

where $\langle u \rangle = 0$ if $u<0$ and $\langle u \rangle = u$ if $u > 0$ and where $\sigma_c = \text{Min} \left\{ \sigma_c^*, \sigma_c(t,T) \right\}$.

σ_c^* is the critical fracture stress of the virgin material and $\sigma_c(t,T)$ that of the embrittled material which is defined by Eq.2 as :

$$\sigma_c(t,T) = \sigma_{co}(T) \times [1 - u(T) + u(T).\exp(m.\lambda/lox)] \qquad (4)$$

Eq.4 involves the depth of interdendritic oxide lox. Metallographic measurements on specimens exposed at various temperatures have shown that the oxide depth lox, could be given by [Reuchet and Rémy, 1983] :

$$dlox = 0.25.lox^{-3}.\alpha_c^4.dt \qquad (5)$$

where α_c is an oxidation constant.

The number of cycles to break down a microstructural element could be given by the critical condition as :

$$\int_0^{N(\lambda)} dD = 1 \qquad (6)$$

The application of this model to thermal fatigue loading conditions is straigthforward, at least in principle. This requires knowing the variation of the interdendritic oxide depth, lox, as a function of time and temperature. For thermal fatigue loading conditions, Eq.5 has to be integrated over a complete thermal cycle. A cycle by cycle computation of Eq.5 can be made until the critical condition of Eq.6 is fulfilled. As the parameters of Eq.3 are temperature dependent, application of this equation needs an equivalent temperature to be defined. As the details of damage cumulation within a cycle period are unknown, this temperature could be either the temperature of the maximum stress or the temperature of the minimum stress. For a pure thermal fatigue loading situation this corresponds to the thermal shocks on cooling and on heating respectively. Therefore $N(\lambda)$ was defined as the geometric mean of the values which were computed in each hypothesis.

Application of this model to thermal fatigue is shown in Fig.8 which compares predicted and experimental crack growth curves for two different maximum cycle temperatures. A good agreement is actually observed between prediction and experiment up to crack length of a few mm. The model is thus able to account for very high crack growth rates and for the decrease in growth rates with increasing crack length.

CONCLUSIONS

An oxidation fatigue damage model has been proposed to account for crack growth in Mar M509 superalloy under isothermal fatigue at high temperature and thermal fatigue.

This model uses a local stress approach to describe the superposition of fatigue and monotonic fracture in a volume element 100μm in size ahead of the crack tip at high crack growth rates. The interaction between oxidation

and fatigue is accounted for through the decrease of the critical stress for monotonic fracture which is induced by oxygen diffusion. This model involves mechanical parameters which are fitted to isothermal experiments on virgin or preoxidized CT specimens and interdendritic oxidation kinetic data which are measured by quantitive metallography. The number of cycles to break a volume element at the crack tip is given by a cycle by cycle computation.

This model accounts for the growth law of thermal fatigue cracks in wedge specimens up to a few millimeters using a stress analysis of uncracked specimens.

ACKNOWLEDGEMENTS

This work is part of a research project which has been funded by the French Ministry of Industry (D.D.S.T.I.) within the European Community COST 50 programm. MM. Y. Honnorat and Aubert from the Materials and Processes Departement of SNECMA have kindly provided access to their fatigue testing facilities for completion of this work.

REFERENCES

Beremin, F.M., (1983). Metall. Trans., A, 14A, 2277-87.

Chalant, G. and Rémy, L., (1983). Eng. Fracture Mechanics, 18, 939-952.

Coffin, L.F., (1973). Fatigue at Elevated Temperatures, ASTM STP 520, American Society for Testing and Materials, Philadelphia, 5.34.

Fischer, J.C., (1951). J. Appl. Phys., 22, 74, Knott, J.F., (1973).

Knott, J.F., (1973). Fundamentals of Fracture Mechanics, Butterworths, London, 251-256.

Mc Clintock, F.A., (1963). Fracture of Solids, D.C. Drucker and J.J. Gilman Eds., Interscience, New-York, 65-102.

Manson, S.S., (1973). Fatigue at Elevated Temperature, ASTM STP 520, American Society for Testing and Materials, Philadelphia, 744-782.

Rémy, L., Rézai-Aria, F., Danzer, R., and Hoffelner, W., (1988). Low Cycle Fatigue, ASTM STP 942, H.D. Solomon, G.R. Halford, L.R. Kaisand and B.N. Leis, Eds. American Society for Testing and Materials, Philadelphia, 1115-1132.

Reuchet, J. and Rémy, L., (1983). Metall. Trans. 14A,141-149.

Rézai-Aria, F., (1986). These d'Etat, University of Paris, Orsay.

Rézai-Aria, F., Dambrine, B. and Rémy, L., (1988 a). Fatigue Fract. Engng. Mater. Struct., 11, 291-302

Rézai-Aria, F., François, M. and Rémy, L., (1988 b). Fatigue Fract. Engng. Mater. Struct., 11, 277-289.

Tracey, D.M., (1976). J. Eng. Materials and Technology, Trans., ASME, 98, 146-151.

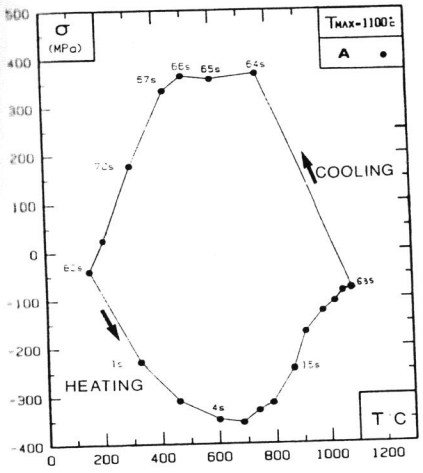

Fig. 1 : Thermal stress for a critical element in a wedge specimen as a function of temperature (Thermal cycle between 200 and 1100°C; time in seconds is indicated along the loop).

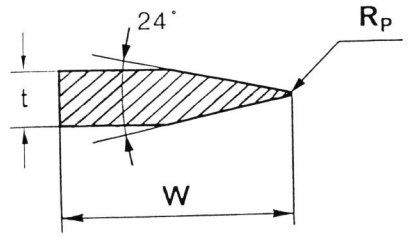

TYPE	W (mm)	R_p (mm)	t (mm)
A	27.60	0.25	6.7
LENGTH 55 (mm)			

Fig. 2 : Cross-section of the 55mm long thermal fatigue specimen.

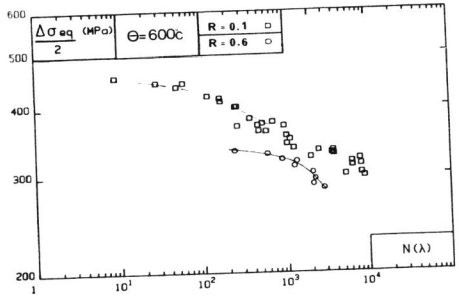

Fig. 4 : Variation of the equivalent stress range in a volume element ahead of the crack tip ($\Delta\sigma_{eq}$) as a function of number of cycles to break it [N(λ)] at 600°C.R is the load ratio.

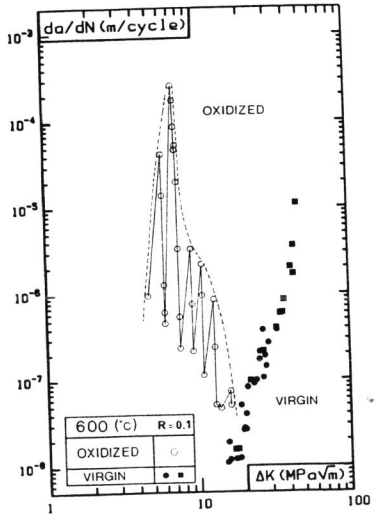

Fig. 3 : Variation of fatigue crack growth rate (da/dN) as a function of stress intensity range (ΔK) at 600°C for a load ratio R of 0.1 for a virgin specimen and for an oxidized specimen.

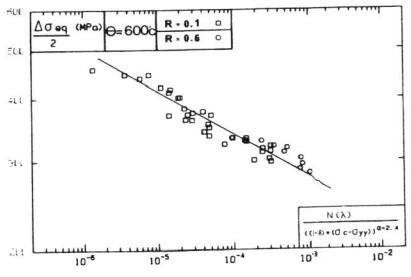

Fig. 5 : Variation of the equivalent stress range in a volume element ahead of the crack tip ($\Delta\sigma_{eq}$) as a function of the ratio $N(\lambda)/[(1-R) \times (\sigma_c - \sigma_{yy})]^{\alpha}$ at 600°C.

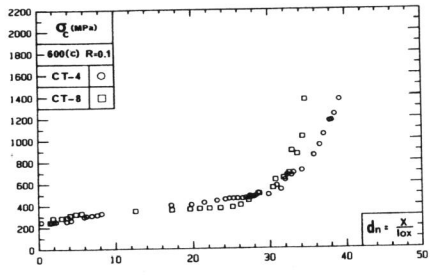

Fig. 6 : Variation of the critical stress to fracture (σ_c) with distance to the tip of oxidized precrack (X) normalized by the interdendritic oxide depth (X/l_{ox}) at 600°C.

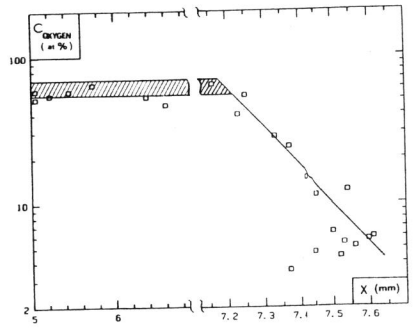

Fig. 7 : Variation of the oxygen concentration (c) ahead of crack oxidized at 900°C (300h) with the distance from the mechanical notch.

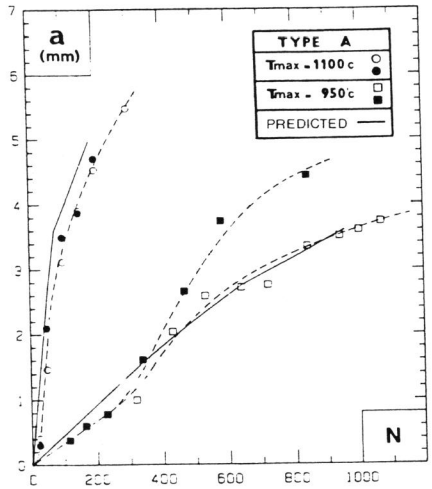

Fig. 8 : Variation of major crack depth with the number of TF cycles in wedge-type specimens. Comparison between experiment (dashed lines) and prediction (solid lines).